

*ARMY RESEARCH LABORATORY*



## **Instrumented Indentation of M855 Cartridge, Core, and Jacket Materials**

**by Mark R. VanLandingham, Thomas F. Juliano, and Matthew J. Hagon**

---

**ARL-TR-3570**

**August 2005**

## **NOTICES**

### **Disclaimers**

The findings in this report are not to be construed as an official Department of the Army position unless so designated by other authorized documents.

Citation of manufacturer's or trade names does not constitute an official endorsement or approval of the use thereof.

Destroy this report when it is no longer needed. Do not return it to the originator.

# **Army Research Laboratory**

Aberdeen Proving Ground, MD 21005-5069

---

---

**ARL-TR-3570**

**August 2005**

---

## **Instrumented Indentation of M855 Cartridge, Core, and Jacket Materials**

**Mark R. VanLandingham, Thomas F. Juliano, and Matthew J. Hagon**  
**Weapons and Materials Research Directorate, ARL**

REPORT DOCUMENTATION PAGE			Form Approved OMB No. 0704-0188		
Public reporting burden for this collection of information is estimated to average 1 hour per response, including the time for reviewing instructions, searching existing data sources, gathering and maintaining the data needed, and completing and reviewing the collection information. Send comments regarding this burden estimate or any other aspect of this collection of information, including suggestions for reducing the burden, to Department of Defense, Washington Headquarters Services, Directorate for Information Operations and Reports (0704-0188), 1215 Jefferson Davis Highway, Suite 1204, Arlington, VA 22202-4302. Respondents should be aware that notwithstanding any other provision of law, no person shall be subject to any penalty for failing to comply with a collection of information if it does not display a currently valid OMB control number. <b>PLEASE DO NOT RETURN YOUR FORM TO THE ABOVE ADDRESS.</b>					
1. REPORT DATE (DD-MM-YYYY) August 2005		2. REPORT TYPE Final		3. DATES COVERED (From - To) March 2004–February 2005	
4. TITLE AND SUBTITLE Instrumented Indentation of M855 Cartridge, Core, and Jacket Materials				5a. CONTRACT NUMBER	
				5b. GRANT NUMBER	
				5c. PROGRAM ELEMENT NUMBER	
6. AUTHOR(S) Mark R. VanLandingham, Thomas F. Juliano, and Matthew J. Hagon				5d. PROJECT NUMBER AH80	
				5e. TASK NUMBER	
				5f. WORK UNIT NUMBER	
7. PERFORMING ORGANIZATION NAME(S) AND ADDRESS(ES) U.S. Army Research Laboratory ATTN: AMSRD-ARL-WM-MA Aberdeen Proving Ground, MD 21005-5069				8. PERFORMING ORGANIZATION REPORT NUMBER ARL-TR-3570	
9. SPONSORING/MONITORING AGENCY NAME(S) AND ADDRESS(ES)				10. SPONSOR/MONITOR'S ACRONYM(S)	
				11. SPONSOR/MONITOR'S REPORT NUMBER(S)	
12. DISTRIBUTION/AVAILABILITY STATEMENT Approved for public release; distribution is unlimited.					
13. SUPPLEMENTARY NOTES					
14. ABSTRACT Instrumented indentation was used to estimate the mechanical properties of as-processed materials used in 5.56-mm M855 projectiles. Three indentation tip geometries were used: a Berkovich tip, a 1- $\mu\text{m}$ -radius conical tip with a 90° cone angle, and a 25- $\mu\text{m}$ -radius conical tip also with a 90° cone angle. Because the Berkovich tip geometry is close to that of an ideal pyramid, the resulting measurements of elastic modulus and hardness for homogeneous, isotropic materials exhibited the least amount of scatter compared to the other two tips. For nonisotropic materials, however, the measurements of elastic modulus and hardness using the Berkovich and 1- $\mu\text{m}$ -radius conical tip exhibited large amounts of scatter. These two probes were found to test similar volumes of material that were on the order of the size scale of the material heterogeneities. Thus, the results were a function of the local microstructure rather than being representative of the bulk material. The 25- $\mu\text{m}$ -radius tip was found to provide results for the nonisotropic materials that had small amounts of scatter and that were similar to bulk measurements, indicating that the volume of material being probed was sufficiently large to average out local microstructural effects. Initial efforts were made to provide full stress-strain data from indentation measurements of the brass cartridge case.					
15. SUBJECT TERMS instrumented nano-indentation, small caliber ammunition, green core materials, brass, copper, nylon, tungsten, tin					
16. SECURITY CLASSIFICATION OF:			17. LIMITATION OF ABSTRACT  UL	18. NUMBER OF PAGES  28	19a. NAME OF RESPONSIBLE PERSON Mark R. VanLandingham
a. REPORT UNCLASSIFIED	b. ABSTRACT UNCLASSIFIED	c. THIS PAGE UNCLASSIFIED			19b. TELEPHONE NUMBER (Include area code) (410) 306-0700

---

## Contents

---

<b>List of Figures</b>	<b>iv</b>
<b>List of Tables</b>	<b>v</b>
<b>1. Introduction</b>	<b>1</b>
<b>2. Experimental</b>	<b>3</b>
2.1 Sample Preparation.....	3
2.2 Indentation Testing.....	3
<b>3. Results</b>	<b>7</b>
3.1 Projectile Cores Testing .....	7
3.2 Cartridge Testing.....	11
3.3 Jacket Testing.....	13
<b>4. Summary</b>	<b>15</b>
<b>5. References</b>	<b>16</b>
<b>Distribution List</b>	<b>17</b>

---

## List of Figures

---

Figure 1. Schematic illustration of an instrumented indentation system (a) and corresponding dynamic model (b).....	2
Figure 2. Core (a) and cartridge (b) sample orientation.....	4
Figure 3. Contact area, $A$ , as a function of contact depth, $h_c$ , for the three tip geometries.....	5
Figure 4. Elastic modulus, $E$ , as a function of displacement, $h$ , for fused silica and each of the three tip geometries.....	5
Figure 5. Hardness, $H$ , as a function of displacement, $h$ , for fused silica and each of the three tip geometries.....	6
Figure 6. Typical loading history for an indentation test (a) and illustration of an indentation array pattern (b).....	6
Figure 7. A 25- $\mu\text{m}$ conical array in Pb-Sb (a) and 1- $\mu\text{m}$ conical array in brass (b).....	7
Figure 8. Elastic modulus, $E$ , as a function of displacement, $h$ , for Pb-Sb samples averaged over all orientations for each of the three tip geometries. All error bars signify one standard deviation. ....	8
Figure 9. Elastic modulus, $E$ , as a function of displacement, $h$ , for tungsten-tin samples averaged over all orientations for each of the three tip geometries. ....	8
Figure 10. Elastic modulus, $E$ , (a) and standard deviation of $E$ (b) as a function of displacement, $h$ , for tungsten-nylon samples. Values are based on averages taken over all orientations for each of the three tip geometries. For clarity in (a), only positive error bars are shown for the Berkovich tip data, and no error bars are shown for the 1- $\mu\text{m}$ conical tip data; both positive and negative error bars are shown for the 25- $\mu\text{m}$ conical tip. ....	9
Figure 11. Elastic modulus, $E$ , as a function of displacement, $h$ , for Pb-Sb tested in three different sample orientations using the 1- $\mu\text{m}$ conical tip. ....	11
Figure 12. Hardness gradient in a unfired cartridge cases measured using indentation with a Berkovich tip and a 25- $\mu\text{m}$ conical tip (a), and measured using a Vickers hardness tip and a 2.5-kg load (b). In (a), values averaged over 2.5-mm incremental distances are also shown, and in (b), maximum and minimum values are plotted; in both cases, the lines connecting the data points are meant only to emphasize overall trends. Location was measured from the closed end of the case. ....	12
Figure 13. Examples of stress-strain data for a brass cartridge cases estimated from indentation with a 25- $\mu\text{m}$ conical tip. Values in legend indicate location along the length of the cartridge case as measured from the closed end of the case.....	14
Figure 14. Elastic modulus, $E$ , as a function of displacement, $h$ , for the copper jacket for the Berkovich tip and the 25- $\mu\text{m}$ conical tip averaged over all locations. ....	14

---

## List of Tables

---

Table 1. Summary of elastic modulus,  $E$ , as measured using indentation with three different tip shapes along with values determined from compression and ultrasound testing. ....10

INTENTIONALLY LEFT BLANK.

---

## 1. Introduction

---

System-level numerical models are being developed to provide a scientific framework for design, optimization, and evaluation of current and future small arms systems. These models require input regarding material properties, preferably determined experimentally from the as-processed materials. For 5.56-mm M855 projectiles, thin-walled copper and brass are used for the bullet jacket and cartridge case, respectively, the latter of which is processed with a hardness gradient. The predominant bullet core material is a lead-antimony (Pb-Sb) alloy at roughly a 5:95 weight ratio of Pb to Sb. Due to environmental mandates, alternative material systems are currently being sought to either replace the Pb-Sb core or to produce a new projectile design. Examples of core replacement alternatives are a tungsten particulate-filled nylon and a tungsten-tin metal blend. Measuring mechanical performance of M855 projectile components, however, is difficult using traditional mechanical test methods due to the small dimensions involved. To address this challenge, instrumented indentation techniques can be used.

Instrumented indentation, sometimes referred to as “nano-indentation,” is a technique used for measuring mechanical properties, specifically elastic modulus,  $E$ , and hardness,  $H$ , over micrometer-sized regions of a sample ( $I$ ). A general schematic of an instrumented indentation system based on a NanoIndenter XP (MTS Systems Corp.) is shown in figure 1a (2). For this system, force ( $P$ ) is controlled electromagnetically – an electrical current is passed through a coil that resides within a round magnet, such that the current passing through the coil is directly proportional to  $P$ . Displacement ( $h$ ) is measured relative to the load frame using a 3-plate capacitive element. The outer plates are fixed to the load frame and the middle plate is attached to the indenter shaft or load train, such that the difference in voltage between the middle plate and the two outer plates is proportional to  $h$ .

Force-displacement ( $P$ - $h$ ) curves produced by instrumented indentation systems are generally analyzed according to the work of Doerner and Nix (3) and Oliver and Pharr (2). Their analyses were in turn based upon relationships developed by Sneddon (4) for the penetration of a flat elastic half space by different probes with particular axisymmetric shapes (e.g., a flat-ended cylindrical punch, a paraboloid of revolution, and a cone). These elasticity-based analyses are normally applied to the unloading data of an indentation measurement, assuming the unloading behavior of the material is characterized by elastic recovery only. The resulting values of  $E$  and  $H$  are single values for the maximum applied depth. To obtain  $E$  and  $H$  as a continuous function of depth, dynamic indentation methods have been developed (2) in which a small harmonic load is superposed over the quasi-static load history. This technique allows for a continuous measurement of the contact stiffness,  $S = dP/dh$ , during the entire indentation process using a dynamic model of the system similar to that shown in figure 1b. In this figure,  $K_f$  and  $K_s$  are the

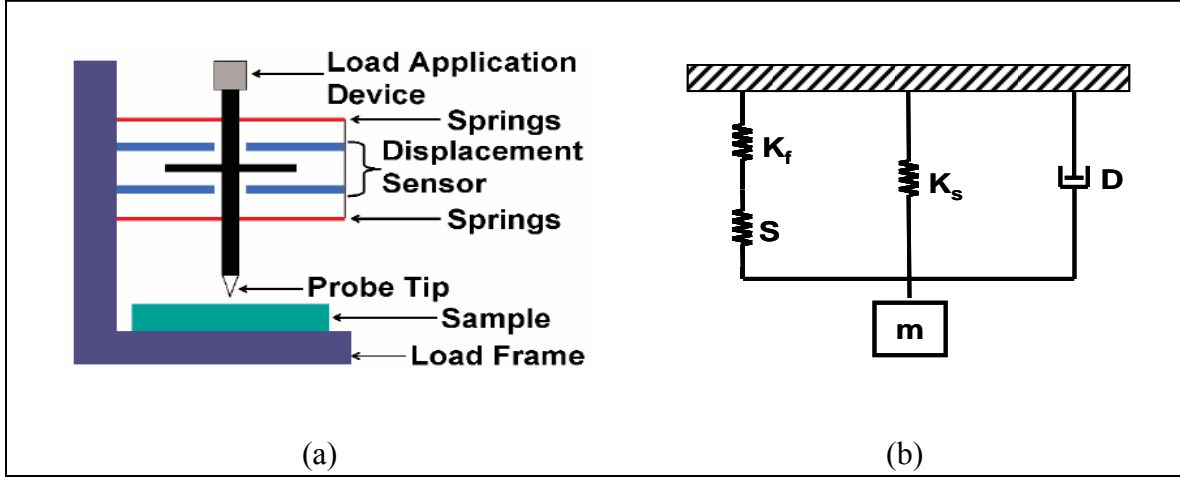


Figure 1. Schematic illustration of an instrumented indentation system (a) and corresponding dynamic model (b).

stiffness of the load frame and column support springs, respectively,  $D$  is the system-damping coefficient, and  $m$  is the system mass. For magnitudes of the force and displacement oscillations,  $P_{os}$  and  $h(\omega)$  where  $\omega$  is the oscillation frequency,  $S$ , can be found from the following equation:

$$\left| \frac{P_{os}}{h(\omega)} \right| = \sqrt{\left\{ \left( S^{-1} + K_f^{-1} \right)^{-1} + K_s - m\omega^2 \right\}^2 + \omega^2 D^2}. \quad (1)$$

Using this method,  $P$ ,  $h$ , and  $S$  are measured continuously during the test, and the reduced modulus,  $E_r$ , can be calculated as a function of  $h$  using

$$E_r = \frac{S\sqrt{A}}{2\sqrt{\pi}}. \quad (2)$$

The contact area,  $A$ , is a function of the contact depth,  $h_c$ , as defined by the tip geometry, which must be calibrated prior to testing. The following relation is used to determine  $h_c$  (and hence  $A$ ) continuously during the indentation test, where  $\varepsilon$  is a geometric factor usually taken to be  $\sim 0.75$ :

$$h_c = h - \frac{\varepsilon P}{S}. \quad (3)$$

Finally, the sample elastic modulus,  $E$ , is determined from the calculation of  $E_r$  assuming knowledge of the Poisson's ratio for the sample,  $\nu$ , and the Young's modulus and Poisson's ratio,  $E_i$  and  $\nu_i$ , of the indentation tip material (usually diamond):

$$\frac{1}{E_r} = \frac{(1-\nu^2)}{E} + \frac{(1-\nu_i^2)}{E_i}. \quad (4)$$

Additionally, the hardness,  $H = P/A$ , can be determined as a function of  $h$ .

In this report, initial efforts to evaluate current and alternative materials for M855 projectiles using instrumented indentation are described. Sample preparation and testing are detailed in the following section, followed by presentation and discussion of results, which includes comparisons to bulk values where possible.

---

## **2. Experimental**

---

### **2.1 Sample Preparation**

The general sample preparation procedure was as follows:

- As-received bullets were placed into a cup mold using plastic clips to hold them in place,
- A two-part epoxy was mixed and poured into the molds and allowed to cure at room temperature for at least four hours prior to removal of the samples from the molds,
- A 120-grit abrasive pad was used to expose the interior of the bullet, which generally required 15-20 min of grinding on a polishing wheel using water and hand pressure,
- Wet sanding continued using 240-, 320-, 400-, and finally 600-grit abrasives; visual inspection with a light microscope was used between sanding and subsequent polishing steps to ensure that scratches from the previous steps had been removed, and
- $\text{Al}_2\text{O}_3$  or diamond suspensions were then used to progressively polish the surfaces using 12-, 9-, 5-, 3-, and 1- $\mu\text{m}$  particle sizes.

The bullets were positioned in such a way as to allow for testing at various orientations of the core material, as shown in the figure 2a. These positions were chosen so that testing could be conducted on vertically, horizontally, and obliquely oriented core surfaces in order to gain more insight into the degree of anisotropy of the materials. One sample disk was made for each of the following core materials: Pb-Sb, tungsten-tin, and tungsten-nylon. In addition to the bullet cores, indentation testing was also conducted on brass cartridge cases. The as-received cartridges were sectioned longitudinally with a diamond saw to expose a clean surface for testing. The mounting procedure was identical to the bullet core procedure except that only a horizontal orientation was used. The horizontal orientation was chosen so that material property gradients along the length of the cartridge could be investigated. The final sample configuration can be seen in figure 2b.

### **2.2 Indentation Testing**

The indentation system used in this study was a NanoIndenter XP (MTS Systems Corp.). Tests were performed using three separate tip geometries: a Berkovich tip (a 3-sided, triangular-based pyramid), a 1- $\mu\text{m}$ -radius conical tip with a 90° cone angle, and a 25- $\mu\text{m}$ -radius conical tip also

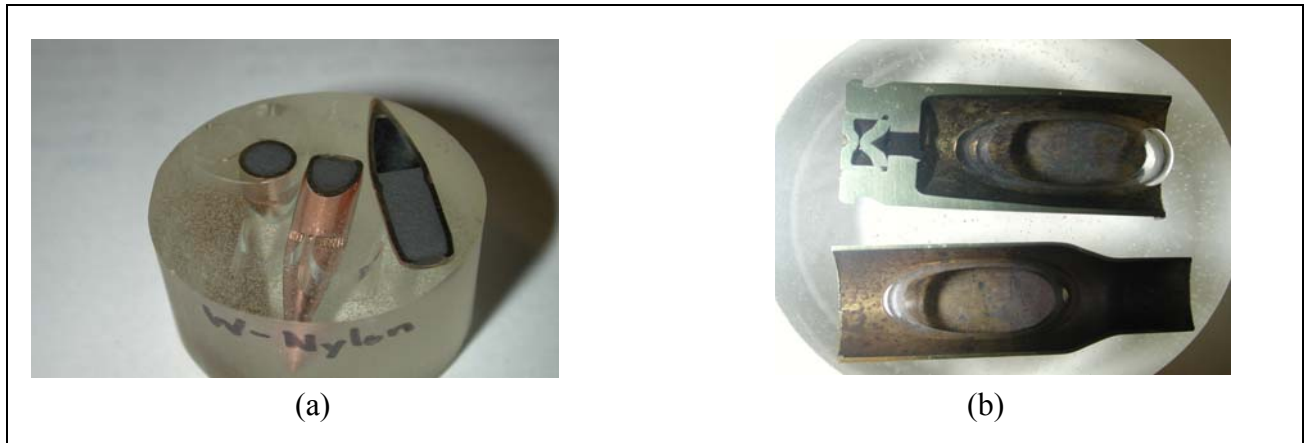


Figure 2. Core (a) and cartridge (b) sample orientation.

with a  $90^\circ$  cone angle. Prior to performing tests on the bullet samples, tip area functions were determined from indentation of fused silica using equations 2 and 3, where reduced modulus is known ( $E_r = 69.5$  GPa), and  $S$ ,  $P$ , and  $h$  are measured such that contact area,  $A$ , can be determined as a function of contact depth,  $h_c$ . Curve fits were then used to provide the indentation software a means to calculate  $A$  as a function of depth for the bullet samples. This data and the associated curve fits are shown in figure 3. For the  $25\text{-}\mu\text{m}$ -radius conical tip, the rounded portion of the tip extends many microns from the tip apex, and thus all indentation performed with this tip can be approximated using spherical contact mechanics. Additional analysis of this tip has shown that it is not a perfect sphere of radius  $25\text{ }\mu\text{m}$ , but rather is slightly more blunt initially with a radius of about  $40\text{ }\mu\text{m}$  which then decreases with distance from the apex, approaching  $25\text{ }\mu\text{m}$  at contact depths of  $600\text{ nm}$  or so. This deviation from ideal geometry, however, should not affect the results significantly.

Modulus and hardness data for fused silica are shown in figures 4 and 5, respectively, for each of the three tips using the respective calibrated area functions. A value of  $E = 74$  GPa is consistently produced for all three tips, except perhaps at small depths where deviations result from measurement uncertainties and artifacts from the curve fits to the area functions, which tend to fit best at larger depths and less so at smaller depths. Hardness values are more sensitive to the tip shape due to the relative amounts of elastic and plastic deformation that the different tip geometries impose as a function of depth. For example, while the Berkovich tip and  $1\text{-}\mu\text{m}$  conical tip create constant hardness conditions for  $h > 400\text{ nm}$ , the  $25\text{-}\mu\text{m}$  conical tip does not create a full plasticity condition at the largest depths obtained.

In figure 6a, the typical loading history used in this testing is shown. For all indentation tests on the samples, the following test sequence was used regardless of tip shape:

- The instrument first approaches and senses the surface.
- After the surface of the material is found, the force is increased using a constant ratio of loading rate to load of  $0.05\text{ s}^{-1}$  until a displacement of  $2000\text{ nm}$  has been reached.

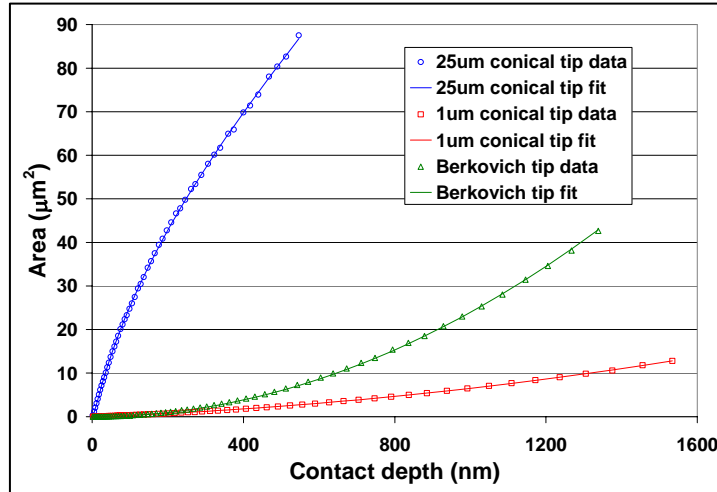


Figure 3. Contact area,  $A$ , as a function of contact depth,  $h_c$ , for the three tip geometries.

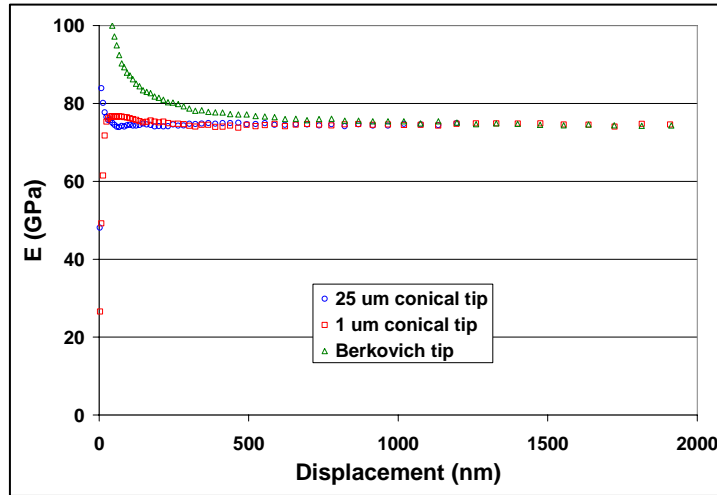


Figure 4. Elastic modulus,  $E$ , as a function of displacement,  $h$ , for fused silica and each of the three tip geometries.

- The load is then held for 10–30 seconds prior to unloading.
- A constant unloading rate is then used to reduce the applied load to 10% of the maximum load, at which point the force is then held constant. This second holding segment is used to correct for the system thermal drift, which will correct for thermal expansion or contraction of the test sample and/or indenter apparatus during the course of testing.

A single series of tests on a given material included 16 or 25 indents equally spaced in a either a  $4 \times 4$  or  $5 \times 5$  square array pattern with a distance of  $40 \mu\text{m}$  between the centers of adjacent indentations. An array of indents is illustrated in figure 6b, where the arrows represent the order in which the tests are performed. Using the optical microscope integrated into the indentation

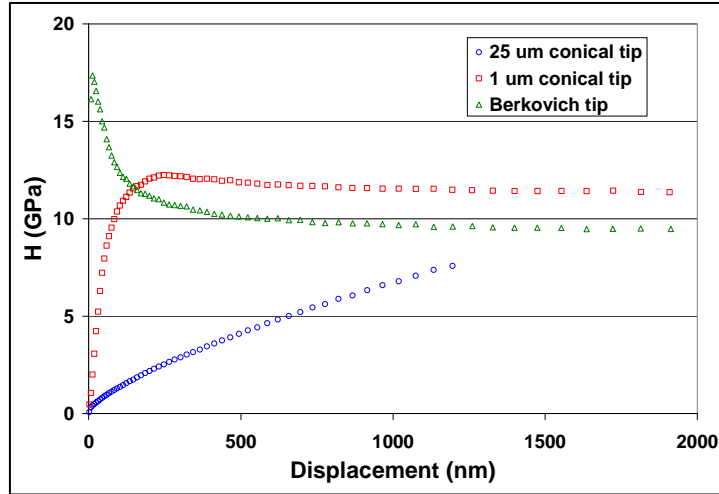


Figure 5. Hardness,  $H$ , as a function of displacement,  $h$ , for fused silica and each of the three tip geometries.

system, locations for the indentation tests were visually selected. Once the tests have been defined, the system automatically moves each of the selected sample positions under the indenter, performing the tests one by one at the specified locations. Optical microscopy images of actual indentation arrays are shown in figure 7. In figure 7a, a  $4 \times 4$  array made using the 25- $\mu\text{m}$  conical tip to indent a Pb-Sb core is shown (scale bar is 20  $\mu\text{m}$  in length), and in figure 7b, a  $4 \times 4$  array made using the 1- $\mu\text{m}$  conical tip to indent a brass cartridge sample is shown (scale bar is 50  $\mu\text{m}$  in length). Poisson's ratio was taken to be 0.3 for brass and 0.4 for all of the core materials.

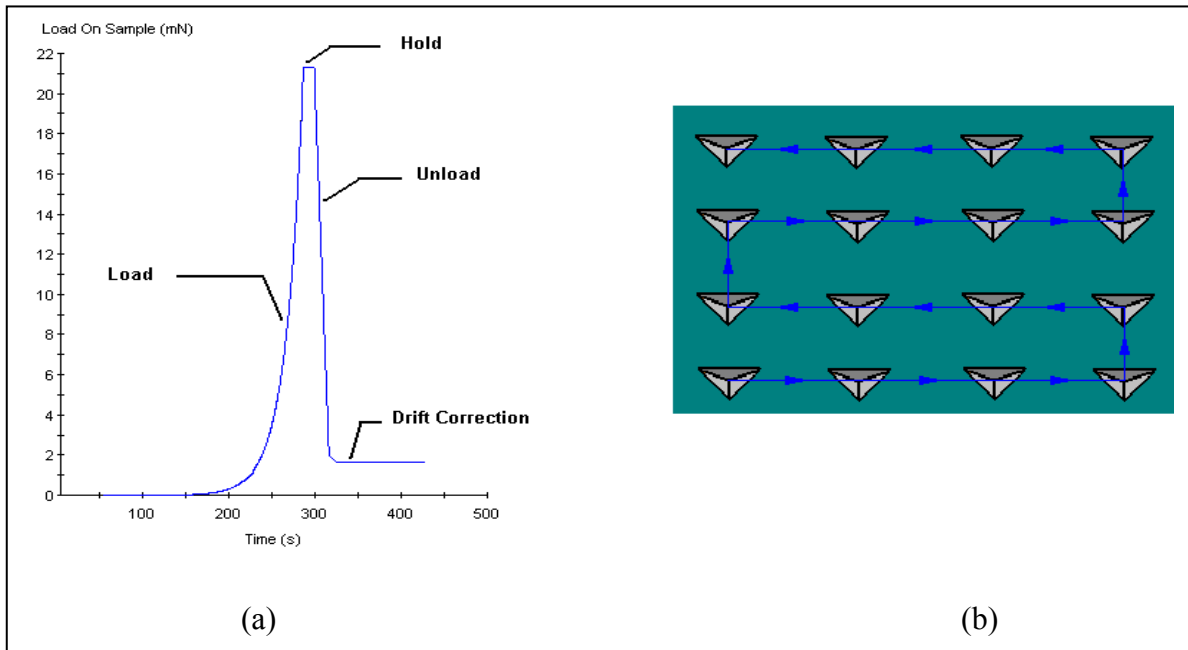


Figure 6. Typical loading history for an indentation test (a) and illustration of an indentation array pattern (b).

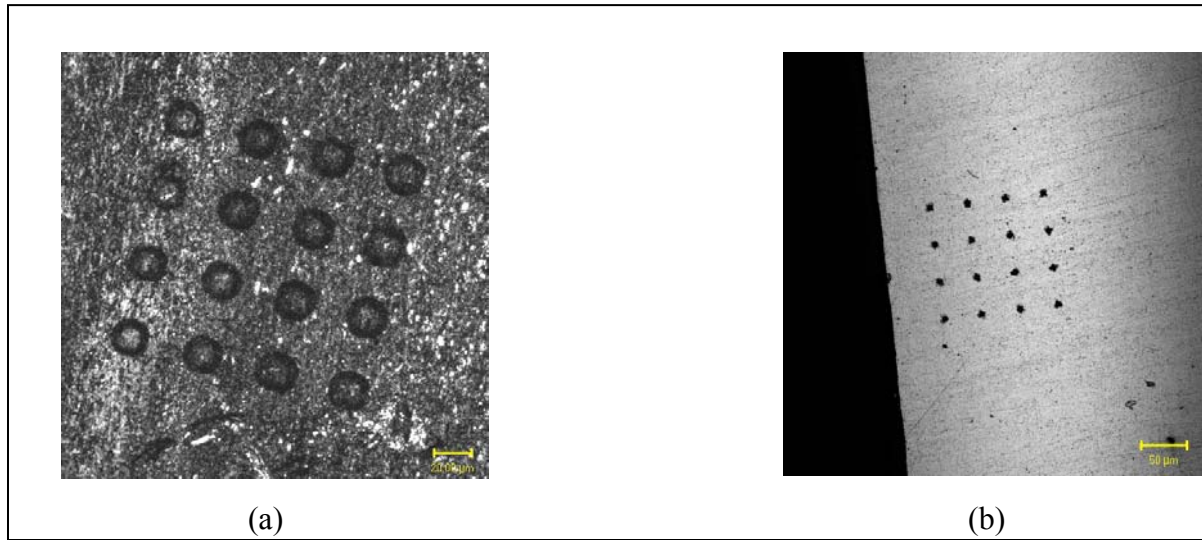


Figure 7. A 25- $\mu\text{m}$  conical array in Pb-Sb (a) and 1- $\mu\text{m}$  conical array in brass (b).

---

### 3. Results

---

#### 3.1 Projectile Cores Testing

In figures 8–10, elastic modulus,  $E$ , is plotted as a function of displacement into the surface,  $h$ , for three core materials – Pb-Sb, tungsten-tin, and tungsten-nylon – as tested with each of the three tip geometries. For  $h > 500$  nm,  $E$  is roughly constant with increasing depth for all three materials. Average values of  $E$  are provided in table 1 along with comparative values for bulk sample testing (compression and ultrasound). Ultrasound testing was used successfully only for Pb-Sb, as this method is only valid for relatively homogeneous samples. Determining  $E$  from compression testing of the actual core materials was also of limited success due to problems with using strain gages on small cylindrical samples (approximate dimensions of 4.6 mm in both length and diameter). Thus, compression modulus values given in table 1 are mainly from samples roughly twice the size of the core materials (approximate dimensions of 9.5 mm in both length and diameter).

Values of  $E$  for Pb-Sb determined from indentation, compression, and ultrasound testing were all approximately 16 GPa, the handbook value for a lightly alloyed Pb material. Further, the values for the three indentation tips were similar within the  $\sim 10\%$  scatter in the data for  $h > 1000$  nm (see figure 8).

The tungsten-tin material was a metal blend  $\sim 60\%$  tin and 40% tungsten by volume, such that no alloying was apparent between the two metal constituents. Tin appeared to comprise the composite matrix with tungsten dispersed as micron-sized islands. Values of  $E$  were only

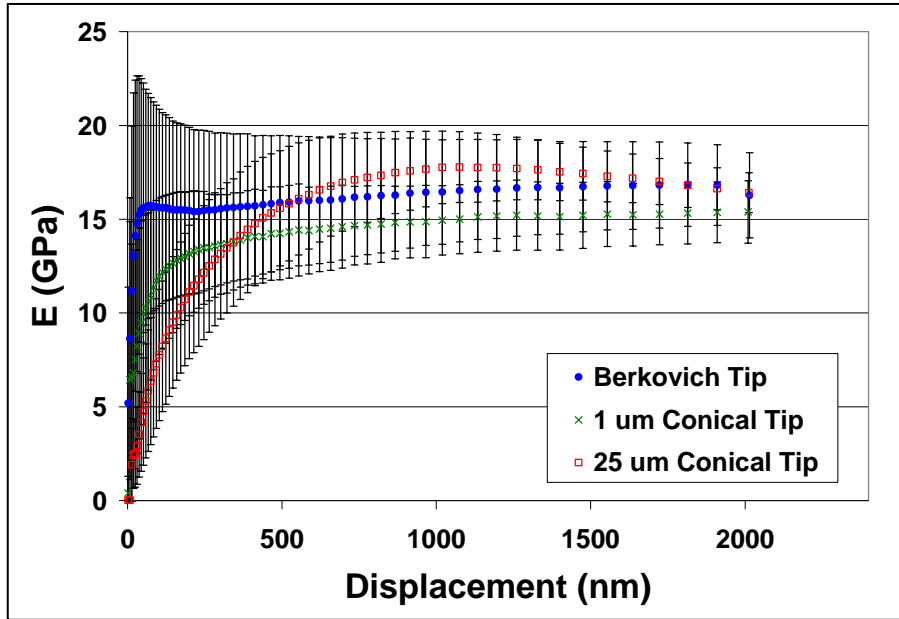


Figure 8. Elastic modulus,  $E$ , as a function of displacement,  $h$ , for Pb-Sb samples averaged over all orientations for each of the three tip geometries. All error bars signify one standard deviation.

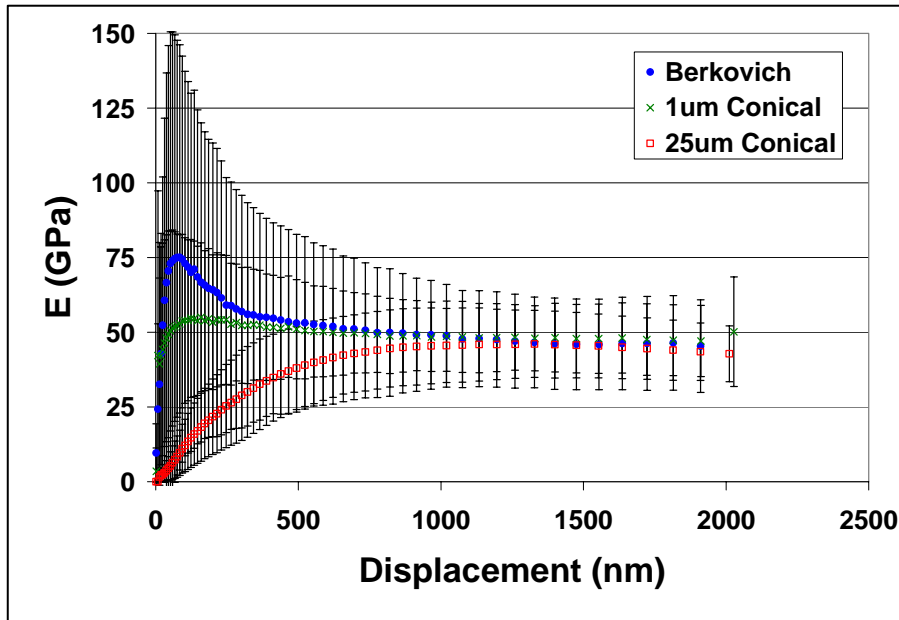


Figure 9. Elastic modulus,  $E$ , as a function of displacement,  $h$ , for tungsten-tin samples averaged over all orientations for each of the three tip geometries.

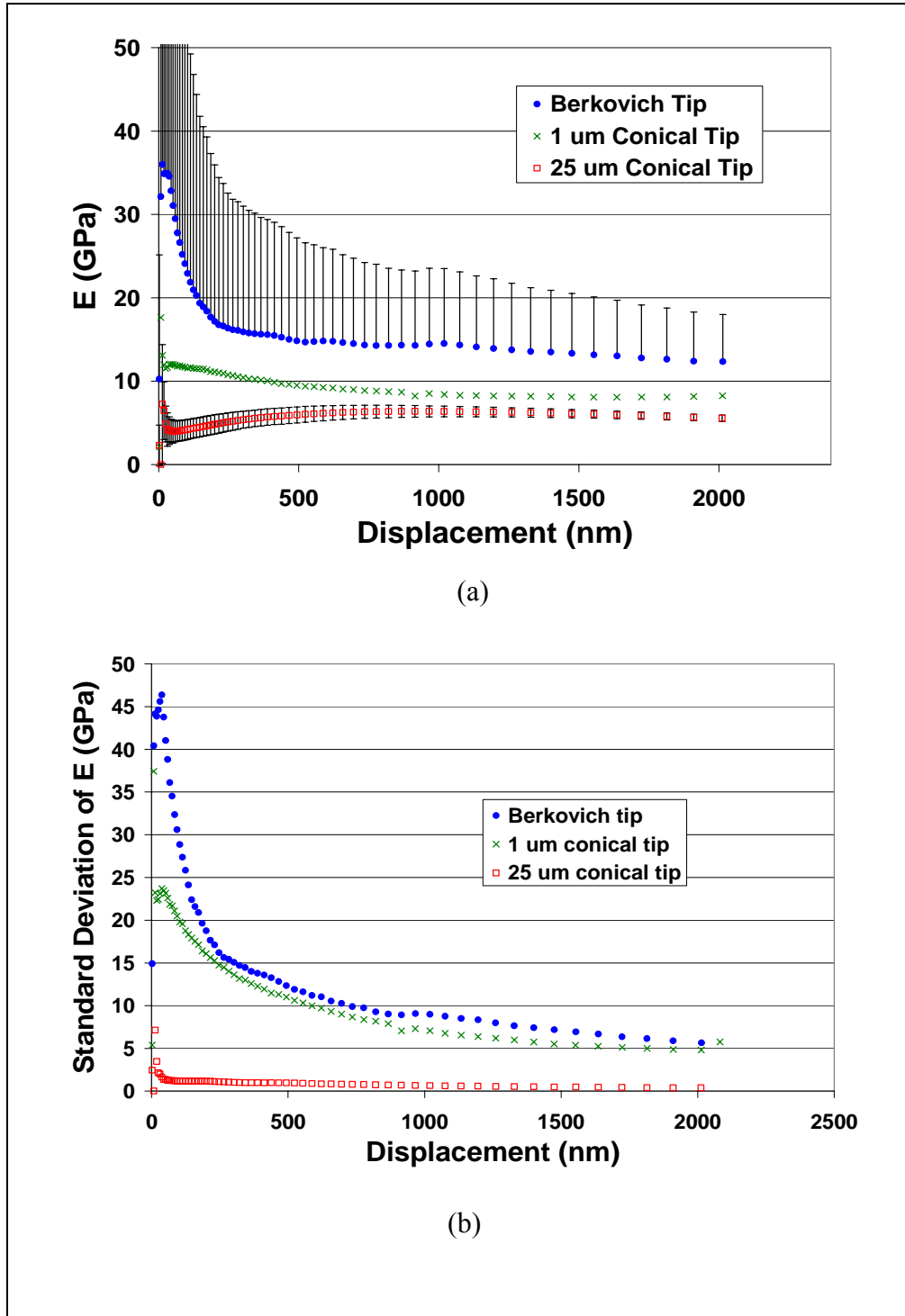


Figure 10. Elastic modulus,  $E$ , (a) and standard deviation of  $E$  (b) as a function of displacement,  $h$ , for tungsten-nylon samples. Values are based on averages taken over all orientations for each of the three tip geometries. For clarity in (a), only positive error bars are shown for the Berkovich tip data, and no error bars are shown for the 1- $\mu\text{m}$  conical tip data; both positive and negative error bars are shown for the 25- $\mu\text{m}$  conical tip.

Table 1. Summary of elastic modulus,  $E$ , as measured using indentation with three different tip shapes along with values determined from compression and ultrasound testing.

Core Material	Indentation $E$ (GPa)			Compression $E$ (GPa)	Ultrasound $E$ (GPa)
	Berkovich	1- $\mu\text{m}$ cone	25- $\mu\text{m}$ cone		
Pb-Sb	$16.7 \pm 2.5$	$15.2 \pm 1.8$	$17.3 \pm 1.5$	$12.0 \pm 2.0$	$14.0 \pm 2.0$
Tungsten-nylon	$13.4 \pm 7.3$	$8.2 \pm 5.8$	$6.1 \pm 0.5$	$9.0 \pm 2.0$	—
Tungsten-tin	$46.8 \pm 15.7$	$48.1 \pm 12.1$	$45.1 \pm 11.0$	—	—

obtained using indentation and were similar to handbook values for tin (42 GPa). Further, the values for the three indentation tips were similar (see figure 9). However, the scatter for all tips was larger than for Pb-Sb, even at large depths where the standard deviation as a percentage of  $E$  was between 20% and 35%. Because the sizes of the tungsten islands were generally in the range of 10's to 100's of microns, data for each of the three tips was sensitive to the local microstructure. In fact, the data scatter tended to be skewed to higher  $E$  values due to the influence of the much stiffer tungsten material ( $E = 410$  GPa). Thus, extracting a representative value of  $E$  for this material from the indentation measurements may not be possible.

The tungsten-nylon material was a Nylon 12 polymer filled with micron sized tungsten particles with a volume fraction of approximately 50%. Using handbook values for the two materials along with micromechanical composite models,  $E$  was estimated to be approximately 10 GPa. However, the presence of voids had been noted in other studies, and as void content increases, the predicted composite modulus decreases substantially. For example, for 3% void volume fraction,  $E$  is reduced by 7%, and for 10% void volume fraction,  $E$  is reduced by 21%. Values of  $E$  measured for tungsten-nylon from compression testing are in general agreement with the micromechanical predictions for a material with 0–10% void-volume fractions. While indentation values were similar to those from compression testing, they were a function of the indentation tip geometry (see figure 10). For the Berkovich tip,  $E$  decreased with  $h$ , approaching 12.5 GPa at  $h \sim 2000$  nm. For the 1- $\mu\text{m}$  conical tip,  $E = 8.2$  GPa for  $h > 900$  nm, and for the 25- $\mu\text{m}$  conical tip,  $E = 6.2$  GPa for  $h > 500$  nm. In figure 10b, the standard deviations for  $E$  are shown to be much smaller for the 25- $\mu\text{m}$  conical tip compared to the other two tips. The average  $E$  values and standard deviations, along with the contact area data in figure 3, indicate that the Berkovich tip and the 1- $\mu\text{m}$  conical tip average over similar volumes of material and thus, the corresponding data is highly sensitive to local microstructure. While the tungsten particle size distribution was quite large, the largest particles were on the order of a few 10's of microns in diameter. Thus, because the 25- $\mu\text{m}$  conical tip probes a much larger volume of material, the data appears to be more representative of the bulk material behavior.

Some evidence was found to suggest some slight anisotropy in some of the samples tested with indentation. In figure 11, a plot of  $E$  as a function of  $h$  for Pb-Sb for different sample orientations is shown. Similar results were also found using the 25- $\mu\text{m}$  conical tip. However, due to the large data scatter, the degree of anisotropy was not clear, and further study of this issue is required.

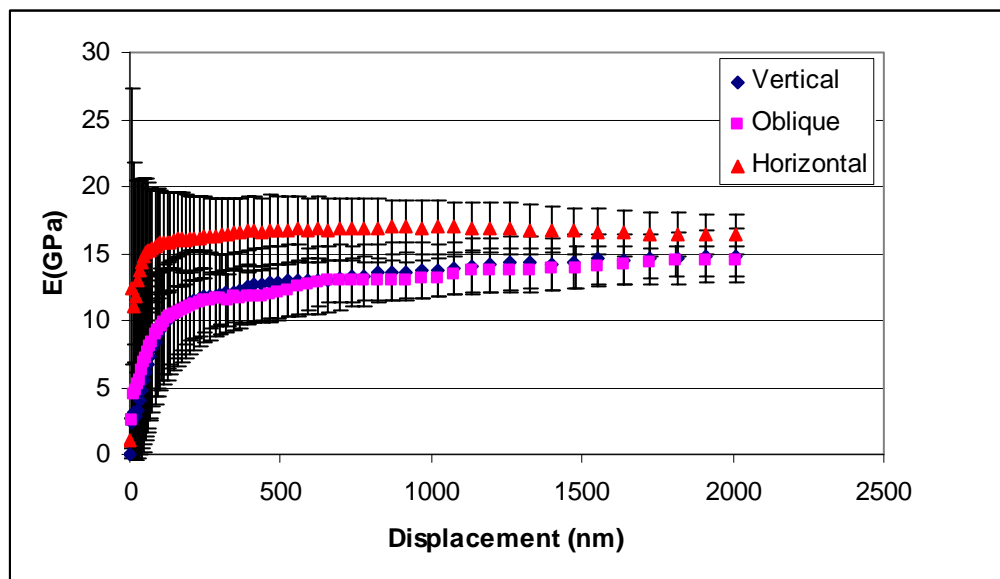


Figure 11. Elastic modulus,  $E$ , as a function of displacement,  $h$ , for Pb-Sb tested in three different sample orientations using the 1- $\mu\text{m}$  conical tip.

### 3.2 Cartridge Testing

Indentation measurements were made on fired and as-processed (unfired) brass cartridge cases as a function of distance along the length of the cartridge using the Berkovich tip and the 25- $\mu\text{m}$  conical tip. For both tips,  $\sim 200$  indentations were made with a spacing of 250  $\mu\text{m}$  along the length of the case, and the resulting values of  $H$  are plotted in figure 12a. The maximum indentation depth for these tests was limited to 500 nm in an attempt to minimize the effects of pile-up known to exist in metals that can overestimate hardness measurements. Also shown in this figure are values averaged over indentations made within approximately a 2.5 mm length along the cartridge case. In figure 12b, a plot of Vickers hardness values measured on a larger scale compared to the instrumented indenter is shown, where data is plotted as maximum and minimum values at each distance tested.

For all data, a similar hardness trend was observed. In general,  $H$  is larger for the lower half of the cartridge case compared to the upper end. Additionally,  $H$  appears to increase slightly (5–10%) with distance for the first 23.5 mm up the cartridge from the base. This increase is followed by a region located between 23.5 and 29 mm from the base where  $H$  drops by 25–30%. The Vickers and 25- $\mu\text{m}$  tip data indicate a gradual decrease ( $\sim 15\%$ ) in  $H$  with distance from 29 mm up to the open end of the case. The Berkovich tip data indicate a slight increase

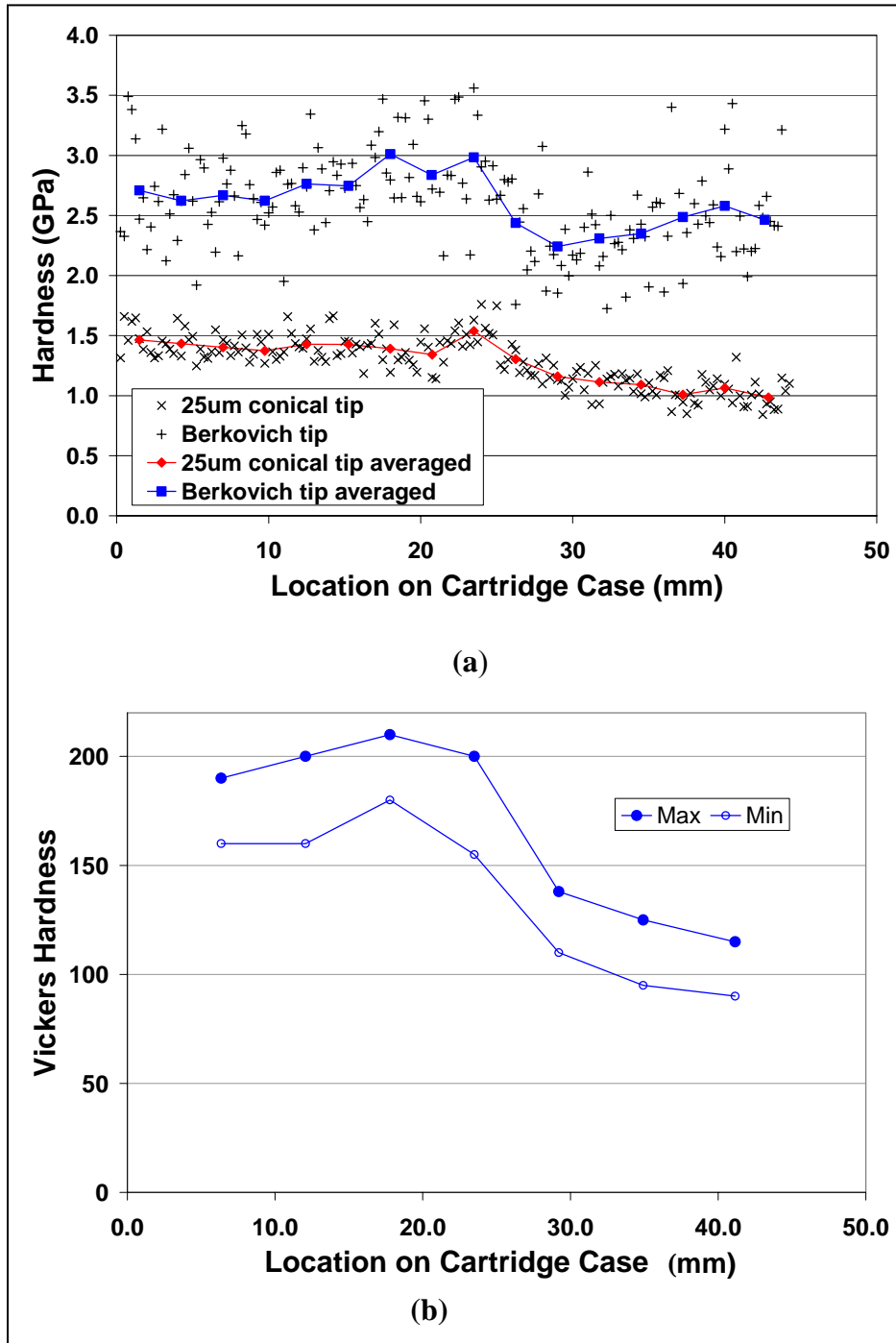


Figure 12. Hardness gradient in unfired cartridge cases measured using indentation with a Berkovich tip and a 25- $\mu\text{m}$  conical tip (a), and measured using a Vickers hardness tip and a 2.5-kg load (b). In (a), values averaged over 2.5-mm incremental distances are also shown, and in (b), maximum and minimum values are plotted; in both cases, the lines connecting the data points are meant only to emphasize overall trends. Location was measured from the closed end of the case.

in  $H$  over the same region. In fact, the 25- $\mu\text{m}$  conical tip seemed to capture the hardness trend better than the Berkovich tip. This result is likely related to the surface roughness, as at  $h = 500 \text{ nm}$ , the contact area of the Berkovich tip is over 10 times smaller than that of the 25- $\mu\text{m}$  conical tip. Also,  $H$  for the 25- $\mu\text{m}$  conical tip was less than that for the Berkovich tip, because spherical indenters will not generate full plasticity in the material until the indenter is of a sufficient depth, whereas sharp Berkovich indenters generate full plasticity just a few nanometers into the surface. However, for all the data, significant amounts of scatter were observed, perhaps indicating significant differences in the brass cases. Also, data for the unfired casing relative to the fired casings were not significantly different; the decrease in hardness occurred perhaps over a slightly larger range. Within scatter, elastic modulus values were constant ( $E \approx 100 \text{ GPa}$ ) along the casings, indicating that the material stoichiometry is constant.

Stress-strain curves were also generated for both a fired and the unfired casing from data taken with the 25- $\mu\text{m}$  radius tool. The stress was taken from the CSM current hardness values, and the strain was taken as the ratio of the measured displacement into the surface to the contact radius,  $a$ , where the contact radius is related to the contact area,  $A$ , by  $A = \pi a^2$ . Examples are shown in figure 13. The stress-strain data did not seem to show any consistent trend as a function of distance along the length of the casing. The material may yield at a higher stress (location where the curve starts to significantly bend) where the overall hardness is higher. This hypothesis would result in an estimation of the yield stress of  $\geq 1 \text{ GPa}$ . However, this value is much higher than handbook values for yellow brass, which range from 97 to 427 MPa. Additional efforts are needed to reconcile these discrepancies.

### 3.3 Jacket Testing

In figure 14,  $E$  is plotted as a function of displacement for the Berkovich tip and the 25- $\mu\text{m}$  conical tip indenting on a polished cross-section of a copper bullet jacket. The values for the 1- $\mu\text{m}$  conical tip (data not shown) were similar to the Berkovich tip. Some slight modulus differences were observed as a function of position, but since no significant variations were expected, the data was averaged from three separate locations on the jacket, and the error bars in figure 14 denote the magnitude of the variations. The values of  $E$  for the 25- $\mu\text{m}$  conical tip were less than those for the Berkovich and 1- $\mu\text{m}$  conical tips. The origin of these differences are not currently known, although it is possible that pile-up of material around the two sharper indenters may have occurred, creating a larger contact area and stiffer contact than accounted for in the analysis, and thus overestimating  $E$ . However, the handbook value for oxygen-free, high-conductivity copper is 125 GPa, with which the Berkovich data is in agreement. Thus, further study is needed to explore these differences.

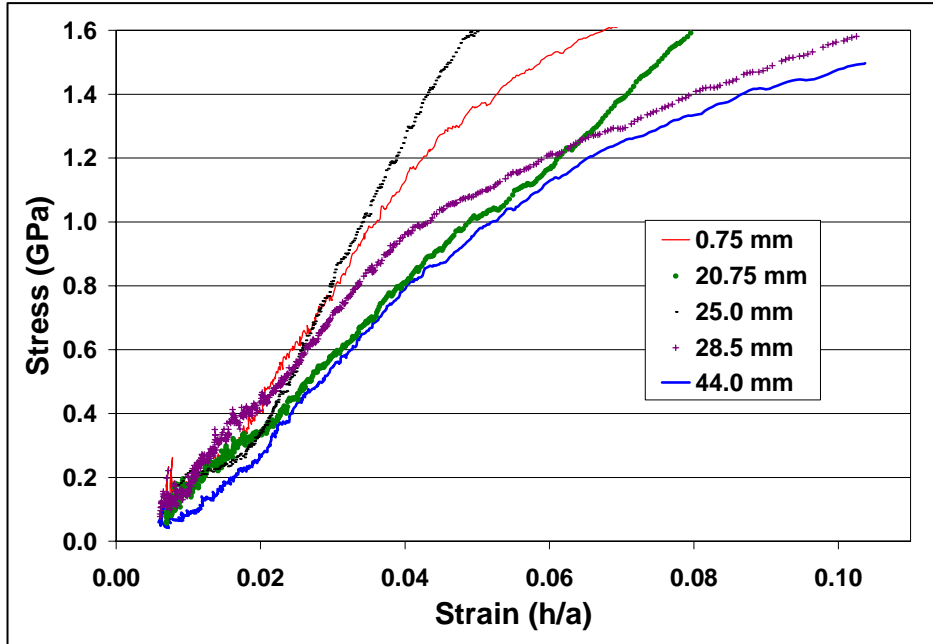


Figure 13. Examples of stress-strain data for a brass cartridge cases estimated from indentation with a 25- $\mu\text{m}$  conical tip. Values in legend indicate location along the length of the cartridge case as measured from the closed end of the case.

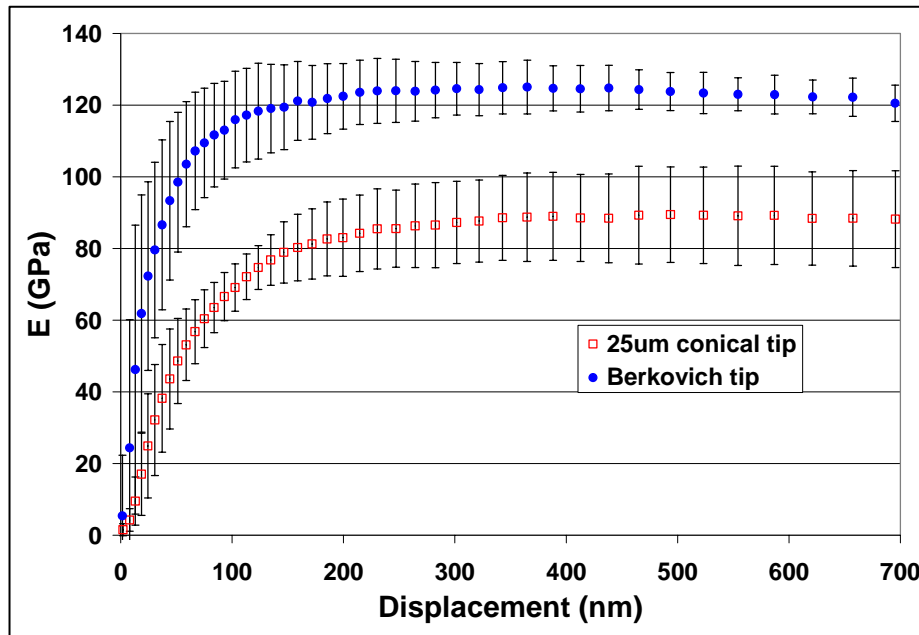


Figure 14. Elastic modulus,  $E$ , as a function of displacement,  $h$ , for the copper jacket for the Berkovich tip and the 25- $\mu\text{m}$  conical tip averaged over all locations.

---

## 4. Summary

---

Instrumented indentation was used to estimate mechanical properties of materials used in 5.56-mm M855 projectiles. Because of the small dimensions of the cores and the small thicknesses of the casing and jacket, indentation was able to provide estimates of elastic modulus for the component materials in an as-processed condition. Three indentation tip geometries were used, including a Berkovich tip, a 1- $\mu\text{m}$ -radius conical tip with a 90° cone angle, and a 25- $\mu\text{m}$ -radius conical tip also with a 90° cone angle. The penetration depths used with the 25- $\mu\text{m}$ -radius conical tip were such that the contact was within the rounded (approximately spherical) part of the tip. This tip was found to provide results for the tungsten particle-filled nylon core material that had small amounts of scatter and that were similar to bulk measurements, indicating that the volume of material being probed was sufficiently large to average out local microstructural effects. Because the Berkovich tip geometry is close to that of an ideal pyramid, the resulting measurements of elastic modulus and hardness for homogeneous, isotropic materials exhibited the most accurate modulus values with the least amount of scatter compared to the other two tips. For nonisotropic materials, however, the measurements of elastic modulus and hardness using the Berkovich and 1- $\mu\text{m}$ -radius conical tip exhibited large amounts of scatter. These two probes were found to test similar volumes of material that were of the order of the size scale of the material heterogeneities. Thus, the results were a function of the local microstructure rather than being representative of the bulk material. Initial efforts to extract full stress-strain data from indentation measurements using the 25- $\mu\text{m}$ -radius conical tip were not successful in providing a reasonable estimation of yield stress.

---

## 5. References

---

1. VanLandingham, M. R. A Review of Instrumented Indentation. *J. Res. Natl. Inst. Stand. Technol.* **2003**, *108* (4), 249–265.
2. Oliver, W. C.; Pharr, G. M. An Improved Technique for Determining Hardness and Elastic Modulus Using Load and Displacement Sensing Indentation Measurements. *Journal Mater. Res.* **1992**, *7* (6), 1564–1583.
3. Doerner, M. F.; Nix, W. D. A Method for Interpreting the Data from Depth-Densing Indentation Instruments. *J. Mater. Res.* **1986**, *1* (4), 601–609.
4. Sneddon, I. N. The Relationship Between Load and Penetration in the Axisymmetric Boussinesq Problem for a Punch of Arbitrary Profile. *Int. J. Engng. Sci.* **1965**, *3*, 47–57.

NO. OF  
COPIES ORGANIZATION

(PDF ONLY) 1 DEFENSE TECHNICAL  
INFORMATION CTR  
DTIC OCA  
8725 JOHN J KINGMAN RD  
STE 0944  
FORT BELVOIR VA 22060-6218

1 US ARMY RSRCH DEV &  
ENGRG CMD  
SYSTEMS OF SYSTEMS  
INTEGRATION  
AMSRD SS T  
6000 6TH ST STE 100  
FORT BELVOIR VA 22060-5608

1 INST FOR ADVNCD TCHNLGY  
THE UNIV OF TEXAS  
AT AUSTIN  
3925 W BRAKER LN STE 400  
AUSTIN TX 78759-5316

1 DIRECTOR  
US ARMY RESEARCH LAB  
IMNE ALC IMS  
2800 POWDER MILL RD  
ADELPHI MD 20783-1197

3 DIRECTOR  
US ARMY RESEARCH LAB  
AMSRD ARL CI OK TL  
2800 POWDER MILL RD  
ADELPHI MD 20783-1197

3 DIRECTOR  
US ARMY RESEARCH LAB  
AMSRD ARL CS IS T  
2800 POWDER MILL RD  
ADELPHI MD 20783-1197

ABERDEEN PROVING GROUND

1 DIR USARL  
AMSRD ARL CI OK TP (BLDG 4600)

NO. OF  
COPIES ORGANIZATION

1 PRODUCT MGR SMALL ARMS  
AND CALIBER AMMO  
SFAE AMO MAS SMC  
M BUTLER  
BLDG 354  
PICATINNY ARSENAL NJ  
07806-5000

1 PROJECT MGR MANEUVER  
AMMUNITION SYS  
SFAE AMO MAS SMC  
R KOWALSKI  
BLDG 354  
PICATINNY ARSENAL NJ  
07806-5000

3 ATK  
R DOHRN MN07-LW54  
C AAKHUS MN07-LW54  
M JANTSCHER MN07-LW54  
4700 NATHAN LANE N  
PLYMOUTH MN 55442

1 ATK LAKE CITY  
K ENLOW  
PO BOX 1000  
INDEPENDENCE MO 64051-1000

5 ATK LAKE CITY  
SMALL CALIBER AMMO  
LAKE CITY ARMY AMMO PLANT  
D MANSFIELD (5 CPS)  
PO BOX 1000  
INDEPENDENCE MO 64051-1000

1 ATK LAKE CITY  
SMALL CALIBER AMMO  
LAKE CITY ARMY AMMO PLNT  
J WESTBROOK  
MO10-003  
PO BOX 1000  
INDEPENDENCE MO 64051-1000

1 ALLIANT TECHSYS INC  
D KAMDAR  
MN07 LW54  
4700 NATHAN LANE N  
PLYMOUTH MN 55442-2512

1 ATK ORDNANCE SYS  
B BECKER  
MN07 MW44  
4700 NATHAN LANE N  
PLYMOUTH MN 55442-2512

NO. OF  
COPIES ORGANIZATION

1 US ARMY TACOM ARDEC  
CCAC AMSTA AR CCL C  
G FLEMING  
BLDG 65N  
PICATINNY ARSENAL NJ  
07806-5000

1 US ARMY TACOM ARDEC  
CCAC AMSTA AR CCL B  
J MIDDLETON  
BLDG 65N  
PICATINNY ARSENAL NJ  
07806-5000

1 US ARMY TACOM ARDEC  
ASIC PROG INTEGRATION OFC  
BLDG 1  
PICATINNY ARSENAL NJ  
07801

1 US ARMY TACOM ARDEC  
M MINISI  
BLDG 65  
PICATINNY ARSENAL NJ  
07806-5000

1 US ARMY TACOM ARDEC  
S SPICKERT-FULTON  
BLDG 65N  
PICATINNY ARSENAL NJ  
07806-5000

1 US ARMY TACOM ARDEC  
M NICOLICH  
BLDG 65S  
PICATINNY ARSENAL NJ  
07806-5000

1 US ARMY TACOM ARDEC  
AMSTA AR CCH A  
S MUSALLI  
BLDG 65S  
PICATINNY ARSENAL NJ  
07806-5000

1 US ARMY TACOM ARDEC  
AMSRD AAR AEM I  
R MAZESKI  
BLDG 65N  
PICATINNY ARSENAL NJ  
07806-5000

NO. OF  
COPIES ORGANIZATION

1 US ARMY TACOM ARDEC  
A FARINA  
BLDG 95  
PICATINNY ARSENAL NJ  
07806-5000

1 US ARMY TACOM ARDEC  
CCAC  
AMSTA AR CCL B  
D CONWAY  
BLDG 65N  
PICATINNY ARSENAL NJ  
07806-5000

1 US ARMY TACOM ARDEC  
CCAC  
AMSTA AR FSF T  
H HUDGINS  
BLDG 382  
PICATINNY ARSENAL NJ  
07806-5000

1 US ARMY TACOM ARDEC  
CCAC AMSTA AR CCL D  
F HANZL  
BLDG 354  
PICATINNY ARSENAL NJ  
07806-5000

1 US ARMY TACOM ARDEC  
P RIGGS  
BLDG 65N  
PICATINNY ARSENAL NJ  
07806-5000

1 OPM MAS  
SFAE AMO MAS MC  
G DEROSA  
BLDG 354  
PICATINNY ARSENAL NJ  
07806-5000

1 COMMANDER  
US ARMY TACOM ARDEC  
AMSTR AR FSF X  
W TOLEDO  
BLDG 95  
PICATINNY ARSENAL NJ  
07806-5000

NO. OF  
COPIES ORGANIZATION

ABERDEEN PROVING GROUND

19 DIR USARL  
AMSRD ARL WM  
S MCKNIGHT  
AMSRD ARL WM BC  
J NEWILL  
S SILTON  
P WEINACHT  
AMSRD ARL WM BD  
P CONROY  
AMSRD ARL WM BF  
W OBERLE  
R PEARSON  
AMSRD ARL WM MA  
M HAGON  
T JULIANO  
P MOY  
M VANLANDINGHAM  
AMSRD ARL WM MB  
J SOUTH  
AMSRD ARL WM TA  
M BURKINS  
S SCHOENFELD  
AMSRD ARL WM TC  
L MAGNESS  
B PETERSON  
AMSRD ARL WM TD  
T BJERKE  
J CLAYTON  
T WEERSASOORIYA

INTENTIONALLY LEFT BLANK.